Numerical Simulation of Three-Dimensional Airflow in Unfurnished Rooms

Trent E. Schulte **Donald J. Bergstrom, Ph.D., P.Eng.James D. Bugg, Ph.D., P.Eng.**

ABSTRACT

This paper considers the numerical modeling of room airflows and illustrates the usefulness of computational fluid dynamics as a design tool for ventilation systems. A computer code, which simulates steady, buoyant, turbulent, three-dimensional flows in Cartesian coordinates, was developed. The time-averaged equations for conservation of mass, momentum, and energy are solved. A low Reynolds number k-ε model is used to simulate the turbulent transport. The code was validated by comparing it to benchmark data for both lid-driven and buoyancy-driven cavity flows. The airflows in two unfurnished rooms were then simulated. Streamlines show that one room is poorly ventilated because a large portion of the incoming air does not pass through the occupied region. The other room has uncomfortable regions because of excessive turbulent fluctuations. Use of computational fluid dynamics enables the velocity and temperature fields to be investigated in significantly greater detail than is possible with either analytical or experimental models.

INTRODUCTION

Buildings are ventilated in order to remove or dilute contaminants, i.e., gases and particulates, and improve the health and comfort of occupants. In addition, the ventilation air is often used to offset the heating or cooling load. Generally, use of lower supply airflow rates and less conditioning of the supply air correspond to reduced operating costs. Ventilation costs can be high when the ventilation air is heated or cooled to meet the room load. Since the 1970s there has been an increasing effort to make buildings more energy efficient by reducing uncontrolled air leakage. However, some of these airtight buildings have exhibited unhealthy levels of air pollutants. In some cases, the solution is as simple as removing the source of contamination. In other cases, however, the problem is inadequate ventilation.

Inadequate ventilation does not necessarily mean insufficient supply airflow rates or too small a supply air temperature differential. Although the supply airflow rate and temperature differential are selected based on the overall heating/cooling load and supply air requirements, the local flow conditions are ultimately determined by details of the flow pattern. Therefore, the ability to predict room airflow patterns is a powerful tool for designing ventilation systems that promote the health and comfort of occupants.

Airflow inside a room is complex. A specific flow pattern is determined by the supply and exhaust locations, room geometry, furnishings, as well as heating and cooling. The flow in most rooms is unsteady, three-dimensional, and buoyant. There can be fully turbulent regions as well as regions with little turbulence. Due to this complexity, there is relatively little information about room airflow patterns available to engineers. Instead, an engineer often must depend on rules of thumb and experience. Since most room configurations are unique, this approach is not always an effective design procedure.

Information on room airflows can be obtained by constructing experimental models and testing them in accordance with *ANSI/ASHRAE Standard 113-1990* (ASHRAE 1990). One problem with physical modeling is that if heating or cooling is involved, the model must be full scale in order to get concurrent equality of the dimensionless inertia, viscous, and buoyancy forces. This can be both costly and time consuming and makes the modeling of large rooms, such as gymnasiums, unfeasible. Given this situation, engineers require an alternative tool that can predict airflow patterns more quickly and less expensively. Computational fluid dynamics (CFD) has the potential to meet these requirements. The cost of a computer simulation is many times lower than the cost of a corresponding experimental investigation, and there is the expectation that computing costs will likely decrease in the future. In addition, numerical modeling of fluid

Donald J. Bergstrom and **James D. Bugg** are associate professors in the Department of Mechanical Engineering, University of Saskatchewan, Saskatoon, Saskatchewan, Canada. **Trent E. Schulte** is a consulting engineer with K.S. Engineering, Inc., Saskatoon.

flows can usually be completed more quickly than a corresponding experimental investigation. However, a CFD simulation of a room airflow is by no means trivial. Furthermore, valid concerns exist regarding the degree of "predictive realism" obtained by numerical simulations using present CFD technology.

Given the above motivation, we offer an example of the application of computational fluid dynamics to prediction of a room airflow. We begin by carefully selecting a turbulence model, in this case a low Reynolds number, two-equation model, which is appropriate for the type of flow being considered, i.e., buoyant recirculating turbulent flow with near-wall regions. Secondly, we implement the mathematical model in a finite volume code that is thoroughly tested to ensure correct application of our numerical method. For benchmark purposes, we choose a number of different reference flows, each of which captures some of the physics important to the room airflow problem. In this paper, we present results that demonstrate that the computational code is capable of accurate prediction of a buoyancy-driven cavity problem for which experimental data are available. Finally, the code is applied to two different hypothetical room configurations. We use two different grid sizes to illustrate that the grid refinement is sufficient to resolve the mean flow features. Having obtained simulation results for the room, we can use them to demonstrate how knowledge of the velocity, temperature, and turbulence fields throughout the room enable the performance of the ventilation system for each room configuration to be evaluated. Our results indicate that the ability to predict details of the flow field can be especially helpful in assessing the performance of a ventilation system.

BACKGROUND

One of the first simulations of room airflow compared measured and calculated mean velocity profiles in a small-scale model room (Nielsen et al. 1978). Velocity measurements were taken using laser Doppler anemometry. The calculated values were obtained using a finite difference solution to the two-dimensional, time-averaged equations for conservation of mass, momentum, turbulence kinetic energy (k), and turbulence dissipation rate (ε). Turbulent transport was modeled using the standard k-ε model with wall functions. Agreement between measured and calculated mean velocity profiles was good, although some discrepancies were found in the area of reverse flow. This was attributed to three-dimensional effects. This work was extended to consider buoyant flows (Nielsen et al. 1979) and three-dimensional flows (Gosman et al. 1980).

With the advent of more powerful computers and numerical techniques in the 1980s and 1990s, the potential to accurately simulate room airflows has increased. Murakami and Kato's research program is representative of current research related to the numerical simulation of room airflows. Murakami et al. (1987) used a standard k-ε model with wall functions to simulate airflows in rooms with no furniture using six different supply and exhaust configurations. The flows simulated had high Reynolds numbers so that the fully turbulent flow assumption of the standard k-ε model was assumed valid in all regions of the room. Also, the flows were isothermal, so the energy equation was not required and buoyancy effects were not incorporated. A passive scalar diffusion equation was included in the code and used to calculate contaminant concentrations for one room configuration. Varying grid sizes were used to illustrate that numerical errors were small. In addition, experimental velocity measurements were taken in identical small-scale model rooms using a tandem type, parallel hot-wire anemometer that could measure velocity components. Flow in the small-scale rooms was visualized using a laser light sheet and magnesium carbonate powder as a tracer. Ethene gas was introduced at several locations in one of the room configurations to act as a contaminant. The gas concentration throughout the room was measured using gas chromatography. Comparison of simulated and measured velocity vectors as well as flow visualization showed good agreement between the simulated and experimental flow patterns. Both the main recirculating flow and secondary flows were well reproduced. Other papers dealing with the numerical simulation of room airflow include Murakami et al. (1989), Murakami et al. (1991), Davidson (1989), and Chen et al. (1992). For a more thorough review of previous numerical simulations of room airflows, see Schulte (1995).

One limitation with some of the previous simulations of room airflow is that they were restricted to two dimensions. The extra degree of freedom given by a third dimension can dramatically change the flow field. Of the simulations that were three-dimensional, many used coarse grids, raising the question of grid dependence of the solutions. As well, some of the three-dimensional flows that were solved were not strongly three-dimensional but instead had one plane of symmetry in the room. Another limitation with many of the previous simulations is that the turbulence models used were dated and in some ways inappropriate. The standard k-ε model with wall functions was used for most simulations. This model assumes that the flow is fully turbulent in all regions of the room. This is not true for most room airflows, which can have regions with very little turbulence. Furthermore, the regions near the walls may not be amenable to treatment by wall functions. The present CFD code addresses the concerns raised above. The code can solve three-dimensional flow problems, so no two-dimensional approximations are required. The room airflows simulated for this paper are strongly three-dimensional. Also, the simulations in this paper were performed using relatively fine grids to enable the grid independence of the solutions to be assessed. Finally, the code uses a low Reynolds number (LRN) k-ε model that is capable of modeling turbulent transport in regions of relatively low-level turbulence. In this sense, the code uses a turbulence model much better suited to room airflows than the high Reynolds number models that were often adopted in the past.

METHOD

A computational fluid dynamics code was developed to solve room airflows. The mathematical model used in the code consists of the time-averaged transport equations for mass, momentum, and energy, as well as transport equations for the turbulence kinetic energy (k) and its dissipation rate (ε). Eddy viscosity model relations are solved for the Reynolds stress and turbulent heat flux.

The k and ε transport equations for a LRN model are generally expressed as follows:

$$\frac{\partial}{\partial t}(\rho k)+\frac{\partial}{\partial x_j}(\rho U_j k)=\frac{\partial}{\partial x_j}\left(\left(\mu+\frac{\mu_t}{\sigma_k}\right)\frac{\partial k}{\partial x_j}\right)+\rho(P_k+G_k-\varepsilon) \quad (1)$$

$$\frac{\partial}{\partial t}(\rho\varepsilon)+\frac{\partial}{\partial x_j}(\rho U_j\varepsilon)=\frac{\partial}{\partial x_j}\left(\left(\mu+\frac{\mu_t}{\sigma_\varepsilon}\right)\frac{\partial\varepsilon}{\partial x_j}\right)+\rho\frac{1}{T}(C_{\varepsilon 1}f_1P_k+C_{\varepsilon 3}G_k-C_{\varepsilon 2}f_2\varepsilon) \quad (2)$$

where U_j is the velocity component, P_k is the shear production, G_k is the buoyancy production, $T = k/\varepsilon$ is the turbulence time scale, ρ is the fluid density, μ is the dynamic viscosity, and μ_t is the eddy viscosity. Here, σ_k, σ_ε, $C_{\varepsilon 1}$, $C_{\varepsilon 2}$, and $C_{\varepsilon 3}$ are model constants, while f_1 and f_2 are damping functions.

The eddy viscosity (μ_t) and eddy conductivity (K_t) relations are as follows:

$$\mu_t=\rho C_\mu f_\mu\frac{k^2}{\varepsilon} \quad (3)$$

$$K_t=\frac{\mu_t}{\sigma_t} \quad (4)$$

where C_μ is a model constant, f_μ is a damping function used in LRN models, and σ_t is the turbulent Prandtl number. The algebraic relations for the Reynolds stress and turbulent heat flux are as follows:

$$\langle u_iu_j\rangle=-\frac{\mu_t}{\rho}\left(\frac{\partial U_i}{\partial x_j}+\frac{\partial U_j}{\partial x_i}\right)+\frac{2}{3}\delta_{ij}k \quad (5)$$

$$\langle u_j\theta\rangle=-\frac{K_t}{\rho C_p}\left(\frac{\partial\theta}{\partial x_j}\right) \quad (6)$$

After experimenting with different LRN formulations, the final model selected was similar to that of Heindel et al. (1994). In this formulation, the damping functions are as follows:

$$f_\mu=\exp\left(\frac{-3.4}{\left(1+\frac{R_t}{50}\right)^2}\right) \quad (7)$$

$$f_1=1.0 \quad (8)$$

$$f_2=1.0-0.3\exp(-R_t^2) \quad (9)$$

where the local turbulent Reynolds number is given by:

$$R_t=\frac{\rho k^2}{\mu\varepsilon} \quad (10)$$

TABLE 1
LRN Model Constants

σ_k	σ_ε	C_μ	$C_{\varepsilon 1}$	$C_{\varepsilon 2}$	$C_{\varepsilon 3}$	σ_t
1.0	1.3	0.09	1.44	1.92	1.44	1.0

The model constants are given in Table 1. Unlike the model of Heindel et al. (1994), $C_{\varepsilon 3}$ is set equal to a constant value. The buoyancy production of ε is difficult to model using an eddy viscosity formulation, so retaining a constant value of $C_{\varepsilon 3}$ is a reasonable approximation for the airflows considered. The boundary conditions at the wall were as follows:

$$k=0 \quad (11)$$

$$\varepsilon=\frac{\mu}{\rho}\frac{\partial^2 k}{\partial x_n^2} \quad (12)$$

The numerical methods used in the code are well-known, standard techniques. The finite volume method of Patankar (1980) is used to discretize the equations. Staggered grids and the upwinding scheme of Raithby and Schneider (1988) are adopted. SIMPLEC (Van Doormaal and Raithby 1984) is used to calculate the pressure field. The time step is included in the discrete equations to act as a relaxation factor in their solution. The equations being solved are nonlinear so the algebraic coefficients must be updated iteratively to achieve a steady-state solution.

The algorithm used in the code to find the steady-state solution fields may be summarized as follows:

1. Find energy equation coefficients.
2. Solve energy equation.
3. Find velocity and pressure correction equation coefficients.
4. Solve velocity and pressure using SIMPLEC algorithm.
5. Find k and ε equation coefficients.
6. Solve k and ε equations.

One iteration of this algorithm constitutes a single time step. The entire algorithm is repeated until a converged solution is obtained. No one parameter was used to determine convergence. Several factors, including the rate of change of the field variables and the residual reduction, were considered, and then a decision was made based upon previous experience. In general, the average normalized residuals of all the equations were reduced by at least four orders of magnitude.

BENCHMARKING

In order to validate the computational code for room airflows, several benchmark flows documented in the literature were solved. These included lid-driven and buoyancy-driven cavity flows, both of which involve turbulent recirculating flow constrained by walls. The benchmark most similar to buoyant room airflow was the two-dimensional buoyancy-driven cavity flow. For this flow, the two vertical walls of a cavity are set at different uniform temperatures while the two

horizontal walls are adiabatic. Air rises along the hot vertical wall and sinks along the cold vertical wall, causing the fluid to circulate. The results of this benchmark calculation are presented below. Refer to Schulte (1995) for further benchmark test results.

Perhaps the most widely referenced experimental study of buoyancy-driven flow in an air-filled cavity is Cheesewright et al. (1986). The cavity had a height of 2.50 m (8.20 ft) and a width of 0.50 m (1.64 ft) with a temperature difference of 45.8°C (82.4°F) between the vertical walls. Detailed velocity and turbulence kinetic energy measurements were taken using laser Doppler anemometry.

The code was used to solve the same flow on a 50 × 50 nonuniform grid, and the simulation results were compared to the experimental measurements. Figure 1 shows the vertical velocity profile along the horizontal line at a height of 1.25 m (4.10 ft). Note the significant effect of turbulence by comparing the experimental and turbulent simulation results to the prediction based on a laminar flow solution. Agreement between the turbulent simulation and the experimental measurements is excellent. The vertical velocity profile along the horizontal line at a height of 0.36 m (1.19 ft) is shown in Figure 2. In both Figures 1 and 2, the maximum discrepancy

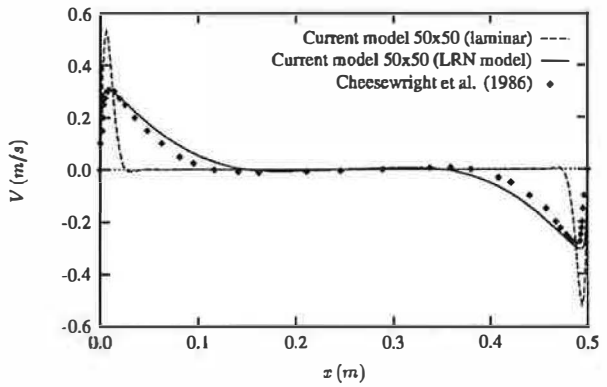

Figure 1 *Vertical velocity along horizontal line at a height of 1.25 m (4.10 ft).*

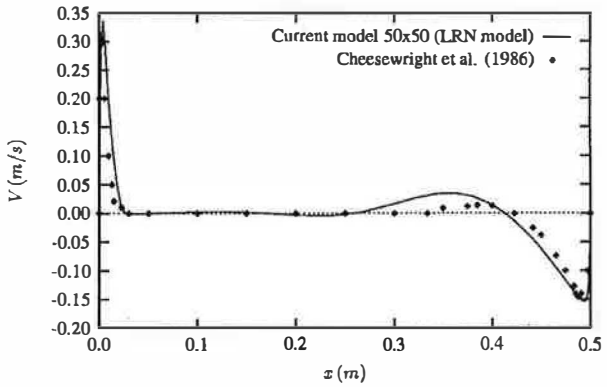

Figure 2 *Vertical velocity along horizontal line at a height of 0.36 m (1.19 ft).*

between the peak values predicted by the code and the experimental measurements was less than 10%. The code predicts the relaminarization of the flow in the bottom corner of the hot wall, which is indicated by the thin boundary layer. Simulation of the turbulence kinetic energy profile along the horizontal line at a height of 1.25 m (4.10 ft) was also excellent. Based upon the successful solution of the benchmark flows, the code was assumed to give reasonably accurate predictions for airflows similar to those encountered in ventilated rooms.

RESULTS

Airflows in a hypothetical unfurnished room were simulated to demonstrate some of the capabilities of the code. The unfurnished room simulated by the code is shown in Figure 3. All surfaces were adiabatic except the east wall and a small section of floor beneath the east wall. The east wall was set to a constant temperature of 15°C (59°F) to approximate an exterior wall during winter, while the section of floor represents a radiator, set to 80°C (176°F), that was used to heat the room. Ventilation air at 20°C (68°F) entered the

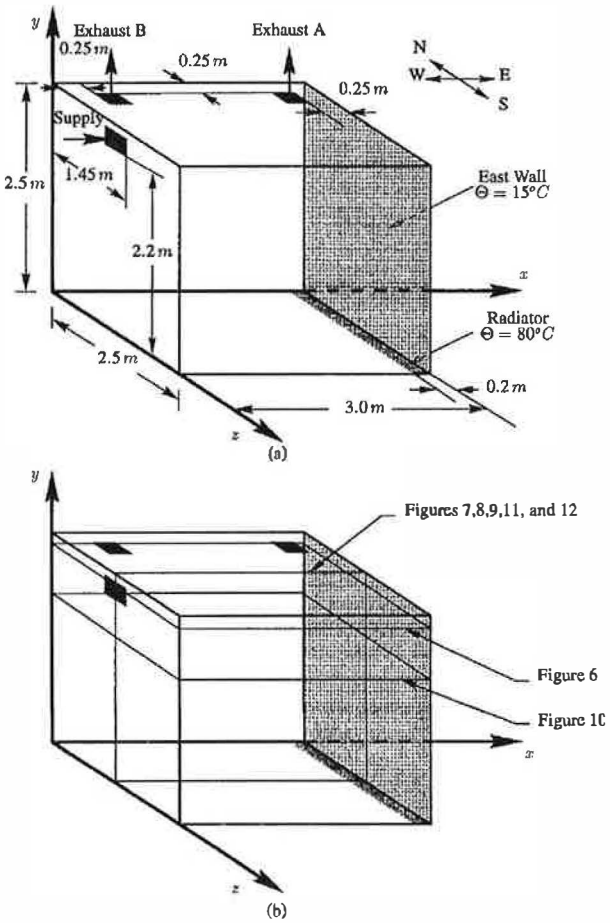

Figure 3 *Details of unfurnished room used in simulations: (a) room dimensions; (b) planes showing locations of other figures.*

room with a velocity of 0.75 m/s (148 fpm) from the 0.40 m × 0.20 m (1.31 ft × 0.66 ft) supply opening in the west wall. Air exited the room through one of the 0.25 m × 0.25 m (0.82 ft × 0.82 ft) exhaust openings. For case A, exhaust opening A was used, while for case B, exhaust opening B was used. Given the room dimensions of 3.00 m × 2.50 m × 2.50 m (9.84 ft × 8.20 ft × 8.20 ft) and the rate that ventilation air was supplied to the room, there were approximately 11 air changes per hour (ACH).

For case A, a 30 × 30 × 30 grid was used, while for case B, both a 30 × 30 × 30 grid and a 50 × 50 × 50 grid were used. Computer storage and the number of calculations required that the 50 × 50 × 50 problem be run on a high-performance platform, in this case a supercomputer. In order to achieve a converged solution, supercomputer times on the order of five hours were required. Solution times could be significantly reduced in the future with changes to the solver to permit higher levels of vectorization. Grids were refined near the supply, exhaust, and walls to provide more accurate simulation in the areas of the greatest gradients. For the 50 × 50 × 50 simulation, the distance between grid points ranged from 0.006 m (0.236 in.) to 0.167 m (6.575 in.).

Boundary Conditions

At the supply opening, the temperature, Θ, and the velocity, U, of the incoming fluid were specified to be uniform. Similarly, k and ε were set uniform over the supply opening. At the exhaust opening, Θ, k, and ε were specified to have zero gradient normal to the opening. The velocity was set uniform over the exhaust opening such that the mass flow rate into the room was equal to the mass flow rate out of the room. For an actual room, it is unlikely that the field variables would be uniform at the supply and exhaust openings. These boundary conditions are recognized as simplifications, and their effect on the flow field remains to be assessed in future studies.

For the 30 × 30 × 30 simulations, 4 × 6 control volumes were used for the supply opening and 3 × 5 control volumes for the exhaust opening. In the 50 × 50 × 50 simulation, 8 × 8 control volumes were used for the supply opening and 5 × 8 control volumes for the exhaust opening.

Streamlines

One method used to visualize the predicted room airflows was streamlines based upon the mean velocity fields. The streamlines were generated using a Lagrangian analysis technique in which the mean path of a fluid parcel is determined by integrating the steady-state velocity fields. Starting from a point at the supply opening, the fluid parcel velocity is calculated by interpolating the velocity field. The fluid parcel at that point is convected through a small time step using the interpolated velocity. At the new position, the velocity is again interpolated and the process is repeated until the fluid parcel exits the room through the exhaust. Several sizes for the time step were tried, and a value of 0.005 s was found to be sufficient to resolve most streamlines. The number of time steps used to go from the supply to the exhaust ranged from approximately 1,500 to 150,000. Due to the coarseness of the grid and inherent inaccuracies in the velocity interpolation, some fluid parcels were found to stop at wall surfaces. In a real flow, the fluid would likely follow the wall surface for some time until it is finally ejected back into the flow. As pointed out by two referees, the use of fluid parcel paths, i.e., streamlines, to infer transport is problematic. For example, a finite fluid parcel would experience diffusive transport—both molecular and turbulent—with the surrounding fluid so that its temperature and composition would vary accordingly along the particle trajectory. We suggest that the utility of the fluid parcel pathlines is as a tool for visualizing the complex flow patterns associated with the three-dimensional field. The associated transport is already calculated in terms of the prediction of the velocity and temperature fields.

Case A

The simulation of case A was performed using a 30 × 30 × 30 nonuniform grid, refined near the supply, exhaust, and walls. To examine this flow, 32 streamlines were calculated starting at various locations in the supply opening. Fourteen streamlines were found to short-circuit, i.e., exit via the exhaust without entering the occupied region of the room, i.e., the region below approximately y = 1.90 m (6.23 ft). The short-circuiting streamlines are shown in side view in Figure 4. The fact that so many of the streamlines short-circuit implies that some of the supply air leaves the room before it has had much time to interact with the surrounding air field. It would be preferable for this air to have a longer residence time in the room, which would enhance the potential for mixing with "old air" in the far corners of the room.

The observation that much of the air that enters the room exits prematurely might suggest that the initial design for the side wall grille was inadequate. However, using the calculation procedure outlined by ASHRAE (1993) the $T_{0.25}$ throw is 5.0 m (16.4 ft) for a generic high sidewall grille. This yields a $T_{0.25}/L$ ratio of 1.7, which is within the recommended range

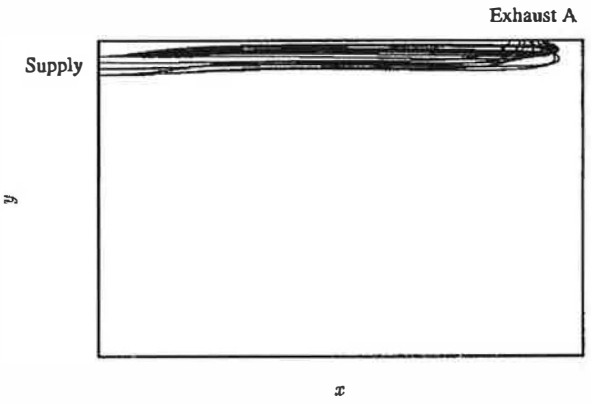

Figure 4 *Side view of short-circuiting streamlines for case A.*

of 1.5 to 1.8 for maximum ADPI. The CFD results presented here illustrate the ability of the technique to predict the behavior of the supply jet including the complexities of the room geometry and exhaust location. The ASHRAE calculations are based on simplified theory for free jets discharging into open environments. Such effects as the presence of a ceiling or wall and the curvature of the supply jet cannot be accurately modeled using these methods. In contrast, CFD enables all of the specific features of the airflow field to be included. The numerical model represents a more accurate prediction for the air diffusion problem than can be accomplished using analytical methods. The computational model correctly shows that for a room configuration with the exhaust located at A, the ventilation system gives poor overall performance. For the given supply air conditions, it was found that improved performance was obtained with the exhaust relocated to location B.

Case B

The simulation of case B was performed using both $30 \times 30 \times 30$ and $50 \times 50 \times 50$ nonuniform grids, refined near the supply, exhaust, and walls. Velocity profiles for various locations in the room were compared to check the grid independence of the solutions. Figure 5 shows the U (horizontal, x) velocity profile at $x = 0.50$ m (1.64 ft), $z = 1.25$ m (4.10 ft). The two simulations agree well, despite the fact that nearly five times as many control volumes are used in the $50 \times 50 \times 50$ simulation. The largest discrepancy in a region of significant flow occurs at $y \cong 0.2$ m (0.66 ft) and is approximately 30%. Over most of the section, the discrepancy is substantially less. Other velocity profiles were also found to agree well. Although strict grid independence is not achieved, both simulation results are of sufficient accuracy to be of practical use in determining the characteristics of the room airflow.

Velocity vector plots were used to study the flow for case B. Figure 6 shows the velocity vectors in the $y = 2.38$ m (7.81 ft) plane. This figure illustrates details of the supply jet behavior that are not apparent in a simple throw calculation but may influence a decision about whether or not this is an effective design. In this case, the simulation reveals significant deflection of the supply jet toward the side of the room with the exhaust opening. Figure 7 shows the velocity vectors in the $z = 1.23$ m (4.04 ft) plane.

Streamlines were also used to study case B. None of the streamlines were found to short-circuit. These streamlines are very complex, and it was impossible to intuitively guess a specific streamline for this flow. However, based upon the streamlines, as well as velocity profiles at various cross sections, some general characteristics of this flow were determined. The supply air travels along the ceiling, moving toward the cool wall and the side of the room near the exhaust opening. The air then flows down along the cool east wall due to both pressure and buoyancy forces. The air circulates back along the floor toward the west wall and then flows up to the exhaust. A fluid parcel may recirculate several times before finally exiting the room.

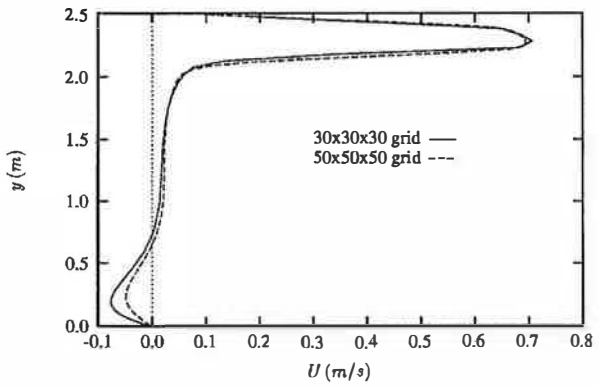

Figure 5 U *velocity profiles for case B at* x = *0.5 m (1.64 ft),* z = *1.25 m (4.10 ft).*

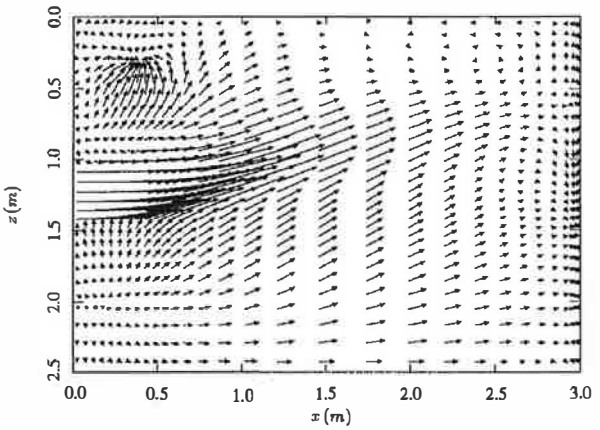

Figure 6 *Velocity vectors for case B in the* y = *2.38 m (7.81 ft) plane.*

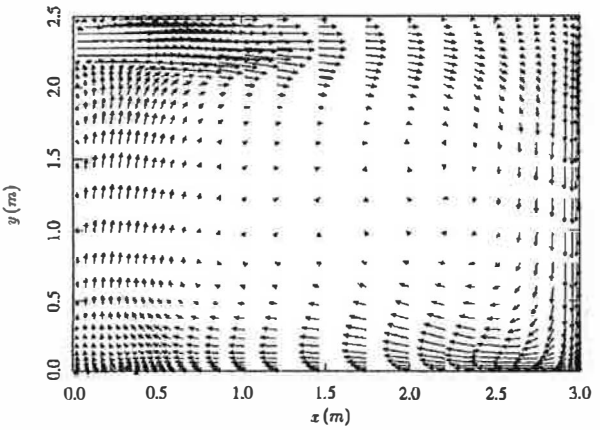

Figure 7 *Velocity vectors for case B in the* z = *1.23 m (4.04 ft) plane.*

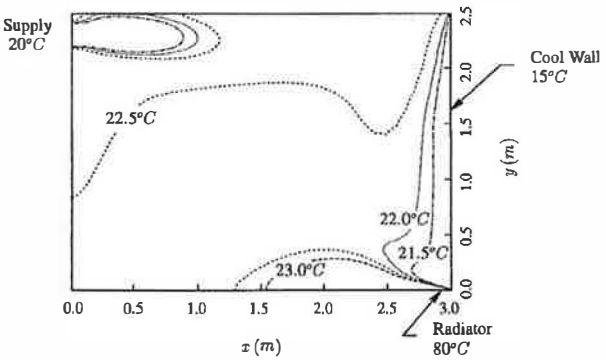

Figure 8 *Mean isotherms for case B at z = 1.25 m (4.10 ft).*

Mean Air Temperature

Figure 8 shows isotherms at a vertical cross section of the room; z = 1.25 m (4.10 ft) based upon the 50 × 50 × 50 simulation fields. This plot and other cross sections at different locations show that the mean temperature in the room lies generally between 21.5°C (70.7°F) and 23.0°C (73.4°F). The air is cooler near the outside wall and warmer near the radiator. The cooler supply air can be seen entering the room in the upper left corner of Figure 8. The temperature range in the room is not large enough to cause discomfort to the occupants. Due to high velocities and turbulent mixing, there is no thermal stratification in the room.

Mean Airspeed

Figure 9 shows the mean airspeed at the same vertical cross section in the room. The *1993 ASHRAE Handbook—Fundamentals* (ASHRAE 1993) states that airspeeds below 0.10 m/s (20 fpm) are not perceived and speeds below 0.25 m/s (49 fpm) are preferred by room occupants. The mean airspeed is above 0.30 m/s (59 fpm) in some parts of the occupied region. A region of excessively high velocity is observed where the supply jet drops into the occupied region. This is illustrated in Figure 10, which shows the mean airspeed at y = 1.76 m (5.79 ft) throughout the room. In the range 2.00 m < x < 2.50 m (6.56 ft < x < 8.20 ft) at approximately z = 0.50 m (1.64 ft), the mean airspeed is above 0.30 m/s (59 fpm). However, the region of the room with an airspeed above 0.30 m/s (59 fpm) is small. Overall, the mean airspeed throughout the room would be noticeable but would not be uncomfortable to most occupants.

Turbulence Intensity

Figure 11 shows turbulence intensity contours for the same vertical cross section of the room. Turbulence intensity is defined as:

$$\text{Turbulence Intensity} = \frac{\sqrt{2k}}{\sqrt{U^2 + V^2 + W^2}} \times 100\% \qquad (13)$$

In the center of the cross section, as well as in the top right and bottom left corners, the turbulence intensity is calculated to be very high because the airspeed is very low. Since the turbulence intensity is normalized in terms of the local mean velocity, in regions of low flow it tends to give high values even though the velocity fluctuations themselves are negligible. However, for the room considered, even in areas with high velocity the turbulence intensity is relatively high. Turbulence fluctuations have a significant impact on the sensation of draft and the comfort of occupants. The high turbulence intensity in this room is found to cause comfort problems as indicated in the next section with the Fanger et al. (1989) comfort equation.

Discomfort Due to Draft

Fanger et al. (1989) developed an empirical equation that estimates the percentage of people who experience discomfort due to draft based upon the air temperature, speed, and turbulence intensity. This relation was chosen over effective draft

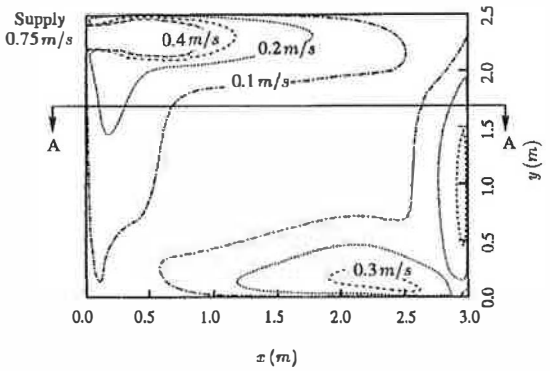

Figure 9 *Mean airspeed contours for case B at z = 1.25 m (4.10 ft). Section AA indicates plane of contours for Figure 10.*

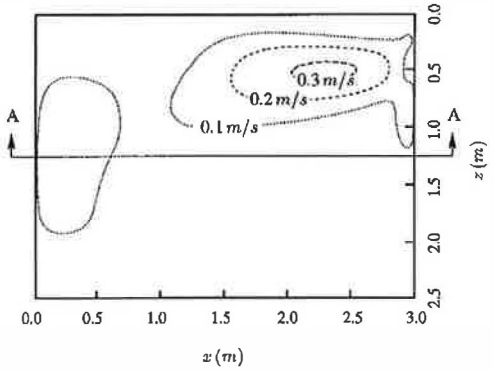

Figure 10 *Mean airspeed contours for case B at y = 1.76 m (5.79 ft). Section AA indicates plane of contours for Figure 9.*

BACK TO PAGE ONE

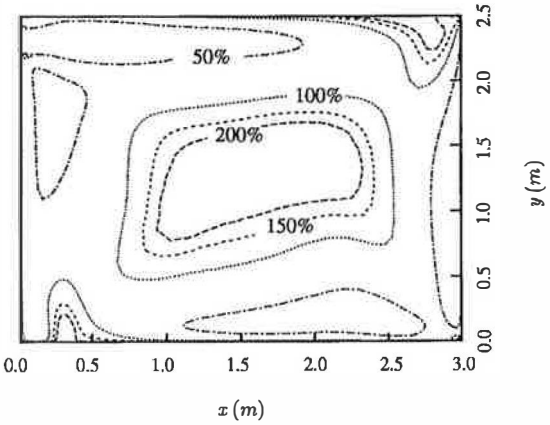

Figure 11 Turbulence intensity contours for case B at z = 1.25 m (4.10 ft).

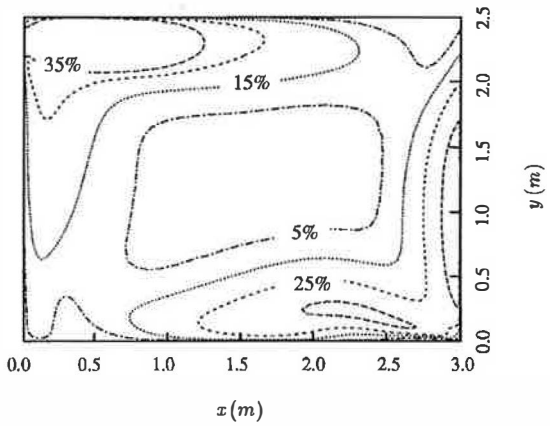

Figure 12 Contours showing percentage of dissatisfied occupants for case B at z = 1.25 m (4.10 ft).

temperature (EDT) because it includes the turbulence intensity. Figure 12 shows contours of the percentage of dissatisfied occupants (PD) at the same vertical cross section of the room. The PD is above 15% in many sections of the occupied region. This is due largely to the high turbulence intensity throughout the room.

Assessment of Case B

Many aspects of the airflow for case B are adequate. From streamlines, it was found that short-circuiting is not a problem. The air temperature throughout the room is satisfactory. The mean airspeed, although it would be noticeable, is satisfactory as well. However, the turbulence intensity is high in many sections of the occupied region, causing discomfort to a high percentage of occupants.

CONCLUSIONS

This paper demonstrates the application of computational fluid dynamics to the analysis of room airflows. Some considerations that are important for such CFD studies include the following:

1. Select a turbulence model that is appropriate for the flow physics to be modeled.
2. In cases where no experimental data are available a priori for comparison, benchmark flows that capture some of the important features of the flow should be used to assess the performance of the code.
3. The numerical accuracy of the final prediction should be investigated using grid refinement.

Although CFD predictions always include errors associated with the many approximations involved, by careful attention to modeling and simulation requirements, these errors can be reduced to a level that enables the results to be used to make valid conclusions regarding room airflow design. In our case, knowledge of the velocity, temperature, and turbulence fields throughout the room enabled the performance of two ventilation systems for a hypothetical unfurnished room to be assessed. This example clearly demonstrates that a significant advantage of CFD over other design tools is that it offers reasonably complete and detailed knowledge of the field variables throughout the room. Simulations can be completed relatively quickly and then used to find a satisfactory ventilation system. For example, the only method that could provide as much information as a $50 \times 50 \times 50$ grid simulation would be detailed experimental measurements at $50 \times 50 \times 50$ points in the room. This would be extremely difficult to accomplish. With the increasing power of computers, numerical techniques, and advances in turbulence modeling, computational fluid dynamics promises to play a larger role in the study of room airflows.

ACKNOWLEDGMENTS

The first author was supported by an NSERC scholarship during this research. Supercomputer time was provided by an HPCC scholarship.

NOMENCLATURE

C_p = specific heat at constant pressure
C_μ, $C_{\varepsilon 1}$, $C_{\varepsilon 2}$, $C_{\varepsilon 3}$ = turbulence model constants
f_μ, f_1, f_2 = damping functions
G_k = turbulent buoyancy production
k = turbulent kinetic energy
K_t = eddy conductivity
L = length of room
P_k = turbulent shear production
PD = percentage of dissatisfied occupants
R_t = local turbulent Reynolds number
T = turbulence time scale
$T_{0.25}$ = throw
U_j = time averaged velocity in the j direction

BACK TO PAGE ONE

u_j = turbulent velocity fluctuation in the j direction
δ_{ij} = Kronecker delta
ε = turbulence dissipation rate
ρ = density
μ = dynamic viscosity
μ_t = eddy viscosity
σ_k, σ_ε = turbulence model constants
σ_t = turbulent Prandtl number
Θ = time-averaged temperature
θ = turbulent temperature fluctuation

REFERENCES

ASHRAE. 1993. *1993 ASHRAE Handbook—Fundamentals.* Atlanta: American Society of Heating, Refrigerating and Air-Conditioning Engineers, Inc.

ASHRAE. 1990. *ANSI/ASHRAE Standard 113-1990, Method of testing for room air diffusion.* Atlanta: American Society of Heating, Refrigerating and Air-Conditioning Engineers, Inc.

Cheesewright, R., K.J. King, and S. Ziai. 1986. Experimental data for the validation of computer codes for the prediction of two-dimensional buoyant cavity flows. *ASME HTD* 60: 75-81.

Chen, Q., A. Moser, and P. Suter. 1992. A numerical study of indoor air quality and thermal comfort under six kinds of air diffusion. *ASHRAE Transactions* 98(1): 203-217.

Davidson, L. 1989. Ventilation by displacement in a three-dimensional room—A numerical study. *Building and Environment* 24: 363-372.

Fanger, P.O., A.K. Melikov, H. Hanzawa, and J. Ring. 1989. Turbulence and draft. *ASHRAE Journal,* April: 18-25.

Gosman, A.D., P.V. Neilsen, A. Restivo, and J.H. Whitelaw. 1980. The flow properties of rooms with small ventilation openings. *Journal of Fluids Engineering* 102: 316-323.

Heindel, T.J., S. Ramadhyani, and F.P. Incropera. 1994. Assessment of turbulence models for natural convection in an enclosure. *Numerical Heat Transfer,* Part B 26: 147-172.

Murakami, S., S. Kato, and H. Nakagawa. 1991. Numerical prediction of horizontal nonisothermal 3-D jet in room based on the k-ε model. *ASHRAE Transactions* 97(1): 38-48.

Murakami, S., S. Kato, and Y. Suyama. 1987. Three-dimensional numerical simulation of turbulent airflow in a ventilated room by means of a two-equation model. *ASHRAE Transactions* 93(2): 621-642.

Murakami, S., S. Kato, and Y. Suyama. 1989. Numerical study on diffusion field as affected by arrangement of supply and exhaust openings in conventional flow type clean room. *ASHRAE Transactions* 95(2): 113-127.

Neilsen, P.V., A. Restivo, and J.H. Whitelaw. 1978. The velocity characteristics of ventilated rooms. *Journal of Fluids Engineering* 100: 291-298.

Neilsen, P.V., A. Restivo, and J.H. Whitelaw. 1979. Buoyancy-affected flows in ventilated rooms. *Numerical Heat Transfer* 2: 115-127.

Patankar, S.V. 1980. *Numerical heat transfer and fluid flow.* New York: Hemisphere Publishing Corp.

Raithby, G.D., and G.E. Schneider. 1988. Elliptic systems: finite-difference method II. *Handbook of Numerical Heat Transfer.* New York: John Wiley & Sons, Inc.

Schulte, T.E. 1995. A numerical model of room airflow. M.Sc. thesis, University of Saskatchewan, Saskatoon, Saskatchewan, Canada.

Van Doormaal, J.P., and G.D. Raithby. 1984. Enhancements of the SIMPLE method for predicting incompressible fluid flows. *Numerical Heat Transfer* 7: 147-163.